THE VISUAL STUDY OF UNSTEADY FLOWS AROUND AN ELLIPTIC CYLINDER PERFORMING ROTATORY OSCILLATION

HANSE, Svein Brendsund
Division of Aero-and Gas Dynamics, The Norwegian Institute of Technology : Research student

Taneda, Sadatoshi
Research Institute for Applied Mechanics, Kyushu University : Professor

https://doi.org/10.5109/6776436

出版情報：Reports of Research Institute for Applied Mechanics. 28 (88), pp.39-55, 1980-09. 九州大学応用力学研究所
バージョン：
権利関係：

Reports of Research Institute for Applied Mechanics
Vol. XXVIII. No. 88, 1980

THE VISUAL STUDY OF UNSTEADY FLOWS AROUND AN ELLIPTIC CYLINDER PERFORMING ROTATORY OSCILLATION

By

Svein Brendsund HANSEN* and Sadatoshi TANEDA**

Results of visual studies are presented for uniform laminar incompressible flow past an elliptic cylinder performing a rotatory oscillation about its trailing edge. The flow patterns and the transient period from start of oscillation to some later time, are studied by means of flow visualization methods in a water tank at Reynolds numbers between 35 and 273 and Strouhal numbers between 0.3 and 2.38.

***Key* words**: : Unsteady flow, Flow visualization, Integrated streakline, Elliptic cylinder

1. Introduction

Viscous flow past an obstacle is one of the basic problems in fluid mechanics. Few areas have received more attention than that of flow past a circular cylinder.

However, there have been presented numerous papers concerning these flow patterns for steady state. Most of the problems related to steady flows are now well understood. Due to the fact that all boundary layers which occur in practice are, in a sense, unsteady, information about unsteady boundary layers and unsteady flow patterns around arbitrary cylinders is very significant to develop the fundamental understanding of fluid mechanics. However, it can hardly be said that the unsteady motions, in general, are well understood so far, but they represent the main trust of the current research efforts.

The flow past an elliptic cylinder is of particular interest because of its fundamental geometry. It is well known that an elliptic cylinder has two extremes, a flat plate and a circular cylinder respectively. Recent studies of

* Research student, Division of Aero-and Gas Dynamics, The Norwegian Institute of Technology, now at Research Institute for Applied Mechanics, Kyushu University.
** Professor, Research Institute for Applied Mechanics, Kyushu University.

flow patterns related to an elliptic cylinder are those by S. Taneda[1], H. Honji[2], H.J.Lugt and H.J.Haussling[3], H.J.Lugt and S.Ohring[4], A.Okajima, H.Takata and T.Asanuma[5] and M.Tatsuno[6].

By means of flow visualization methods in incompressible flow, two basic hydrodynamic lines can be obtained, the streaklines and the streamlines. A streakline is defined as the locus of all particles that have passed through a given point. A pathline is the trace or trajectory of a given fluid particle moving in the flow field. In steady flow, by definition, each particle coming through a given point follows the same trajectory; hence, the streakline and the pathline coincide. Since a streamline is defined as a curve that is everywhere tangent to the velocity vector, say in steady flow, the streamline is everywhere tangent to the pathline and thus coincide with both the pathline and the streakline. However, in unsteady flow the pathline, streakline and streamline differ markedly from each other. It should also be noted that, though the streakline is invariant with respect to the reference frame, the streamline is not invariant, and therefore differ from each other in different frames.

As well known, the separation point in steady state is the point of vanishing of the shear stress at the body. As noted by Moore[7], Rott[8] and Sears[9], the vanishing of the wall shear stress hold no special significance in unsteady boundary layers. They developed a model for unsteady separation point which is known as the Moore-Rott-Sears model, or only MRS model. However, it is not gained full agreement about the definition of unsteady separation point, and there are also many other definitions.

The only possible way to detect the unsteady flow separation is to place tracer particles at the whole surface of the body, and visualize the lines composed of all fluid particles which come out of the whole surface. These streakline patterns have been denoted the "integrated streaklines". As reported by S. Taneda, H. Honji and M. Tatsuno[10], the electrolytic precipitation method is most useful to observe the integrated streakline.

In a recent paper S.Taneda[1] presented, among other things many clear pictures of unsteady flows around an elliptic cylinder performing a rotatory oscillation about its center. He reported that two integrated streaklines were shed from one position located near the trailing edge of the cylinder. The purpose of this paper is to present the integrated streakline flow patterns around an elliptic cylinder performing a rotatory oscillation about its trailing edge and compare these with the work of S.Taneda[1].

2. Apparatus and experimental methods

The experiments were carried out using a water tank 600 cm in length, 50 cm in width and 50 cm in depth. A carriage was run with a constant velocity on rails above the tank. The values of the test cylinder, which was a 2:1 elliptic cylinder attached to the carriage, were ; the major axis

$a=3.0$ cm, the minor axis $b=1.5$ cm, $e=0.866$, the eccentricity e being defined as $e=\sqrt{1-(b/a)^2}$. The focal distance $c=\sqrt{a^2-b^2}$ has the value $c=2.599$. The angular amplitude of oscillation θ was 30° and the mean angle of incidence $\bar{\alpha}$ was 0°. The instantaneous value of θ is denoted as α. The velocity of the carriage could be run with uniform velocity varried from 0 to 30 cm/s. Figure 1 shows the general arrangement of the apparatus.

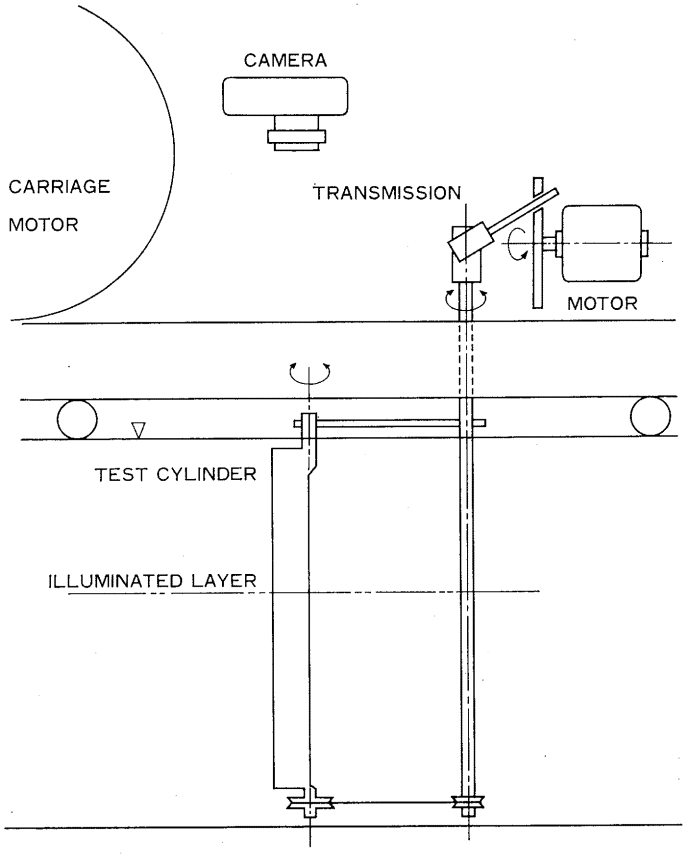

Fig. 1. Schematic diagram of the experimental apparatus.

The photographs of the streamlines and the streaklines around the body were obtained by means of the aluminium powder method and the electrolytic precipitation method respectively. As to the aluminium powder method the central horizontal plane of the water tank was illuminated from both sides, and the movement of the aluminium particles was photographed by a Nikon camera with a 135 mm lens from above. In the electrolytic precipitation method a white colloidal cloud which was generated on the surface of the cylinder

was used as the tracer material. The test body was covered by a metal used as the anode. The intensity of the cloud depended on the metal. Tin emits the thickest cloud and tin solder was used here. The generation of tracer material could be easily regulated by varying the electric supply potential.

An electric motor together with an mechanically operated transmission mechanism was used to obtain the rotatory oscillation. The frequency of oscillation was 0.1 Hz. The Reynolds number was based on the major axis as well as the Strouhal number. Figure 2 shows the mechanically operated transmission mechanism used to obtain the rotatory oscillation. The cylinder oscillation was started after the flow became steady with the elliptic cylinder at the mean position. Figure 3 shows the motion of the test cylinder.

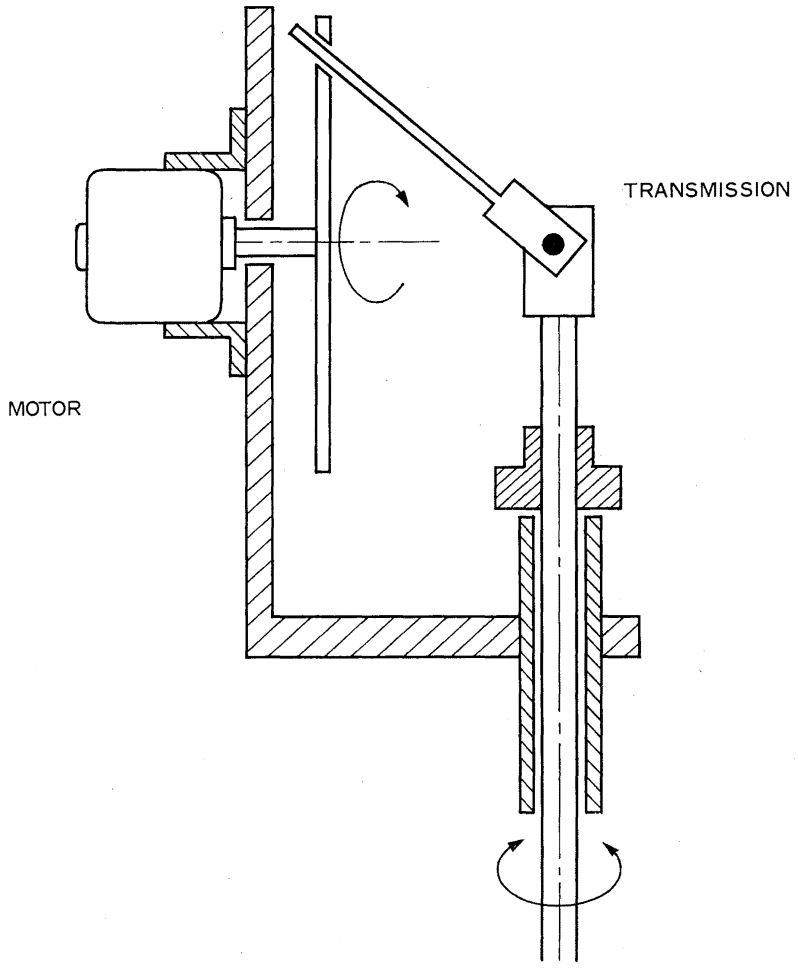

Fig. 2. Mechanically operated transmission mechanism used to obtain the rotatory oscillation.

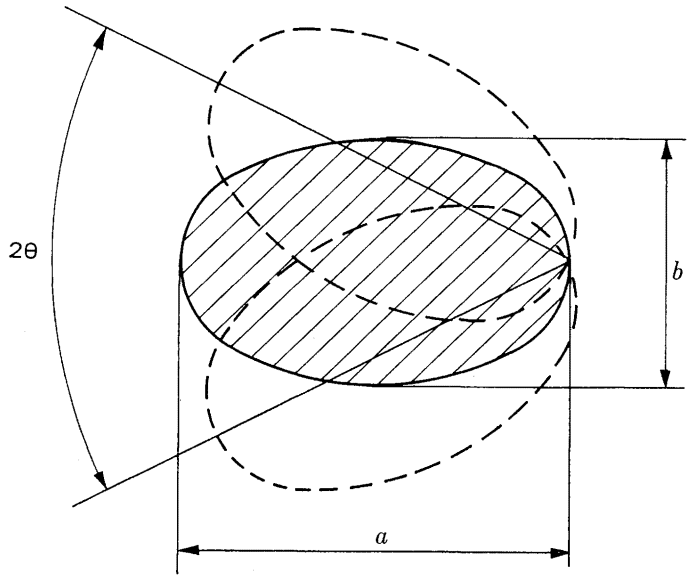

Fig. 3. Motion of the test cylinder.

3. Results of experiments

Figure 4 shows the streamline patterns and the corresponding streakline patterns around a 2:1 elliptic cylinder performing a rotatory oscillation about its trailing edge in water at rest at an oscillation frequency $N=0.1$ Hz. The streamline patterns show two vortices generated upstream of the cylinder. The point where the integrated streakline is shed from the body is oscillating around the leading edge. At the extreme positions the integrated streakline is shed almost from the leading edge. The dye is moved slowly downstream from the cylinder. Downstream is defined as the direction from the leading edge to the trailing edge at the mean position. Also the outer vortex is moved downstream, though very slowly. This should indicate that a slow jet is induced; the direction of the rotation of vortices is opposite to that of vortices in a wake. Therefore it might be expected that there exists a critical frequency at which the jet turns into the wake. It should be noted that an induced jet in downstream direction will cause a thrust.

Figure 5 shows the streamline patterns and the corresponding streakline patterns when a comparatively low free strem velocity is added, $U=0.126$ cm/s. The streamline patterns show that the outer vortex is washed away downstream but the inner vortex is nearly at the same position as in the

case of oscillation in water at rest. However, the streakline patterns show no essential difference. The whole streakline flow patterns are moved a certain distance downstream as compared with that in the case of oscillation in water at rest without undergoing any change in shape.

Figure 6 shows the streamline patterns and the corresponding streakline patterns at a higher value of the free stream velocity, $U=0.259$ cm/s. The streamline patterns show the same vortex generated upstream of the cylinder, but a change in position relative to the cylinder is observed. The vortex is also connected to a stagnation point or a so-called "saddle point" near the leading edge. It should be noted that this stagnation point is not on the surface but at a certain distance from it. Also it should be remembered that the streamline patterns are not invariant with respect to the transformation of the reference frame. However, the velocity of the elliptic cylinder relative to a reference frame fixed to the mean position of the cylinder is nearly 0 at the extreme position of the cylinder. The streakline patterns show that the direction of vortex rotation is reversed. A wake may be formed, but any clear vortex street can hardly be observed. Also here it can be seen that the point where the integrated streakline is shed from the body is oscillating around the leading edge, though without any increase of amplitude. It should be noted that there is no clear correspondence between the saddle point and the integrated streakline.

Figure 7 shows the streamline patterns and the corresponding streakline patterns at $U=0.5$ cm/s. In the streamline patterns it can now clearly be seen that the vortex generated upstream of the cylinder is moved downstream relative to the cylinder due to the increace of the free stream velocity. Otherwise, the streamline patterns do not show any essential difference from that in the previous case. The streakline patterns show now that the direction of vortex rotation has changed to be the same as for the vortex street. There still exists streakline separated from the location immediate to the leading edge, but covers the front region of the cylinder and therefore become complicated ; the streakline patterns make a very small angle with the surface of the body, and this makes it difficult to determine precisely the point where the integrated streakline is shed from the body.

Figures 8.1 and 8.2 show the streamline patterns and the corresponding streakline patterns respectively at $U = 0.76$ cm/s. The streamline patterns show that the vortex generated upstream of the cylinder is moving downstream along the cylinder and is now nearer the trailing edge than the leading edge. It should be expected that this vortex will reach the trailing edge with further increase of the free stream velocity. The streamline patterns show now for the first time a very clear vortex street in the wake of the cylinder. What is very interesting is that this vortex street consists of twin vortices when the elliptic cylinder is at the extreme position. However, the streamline patterns for the flow past the cylinder at the mean position show that the twin vortices are now separated and form a normal vortex

street. The streakline patterns show very clear the vortex street, and also a tail at the trailing edge is clearly visualized. This tail has a very pronounced kink immediately behind the cylinder. The vortex which forms the upper part of the vortex street is shed from the surface of the cylinder when it is at the lower extreme position.

Figure 9 shows the streamline patterns from the start of oscillation to some later time. The free stream velocity is $U=1.0$ cm/s. The streamline patterns show that before the start of oscillation a vortex street is formed in the wake. After sometime the same vortex is generated upstream of the cylinder, but now very near the trailing edge. The wake is changing in time, and after some cycles of oscillation the wake turns into a flow of open streamline patterns. Also the vortex generated upstream of the cylinder disappear at some later time. The streamline patterns are the same at the same phase of the oscillatory motion of the cylinder after a value $x/a=12.5$ is reached, where $x=U\cdot t$.

After this stage twin vortices are formed behind the elliptic cylinder at the extreme position. Also a kink of the streamline patterns behind the cylinder is seen.

4. Conclusions

The results of observations of the integrated streakline patterns and the streamline patterns around an elliptic cylinder performing a rotatory oscillation about its trailing edge have been presented. The main conclusions are as follows:

1) There is no coincidence between integrated streakline patterns and streamline patterns.
2) The saddle point appears in the streamline patterns, but there is no clear correspondence between the saddle point and the integrated streakline.
3) At a comparatively high value of the free stream velocity no vortices appear in the wake after some time, and twin vortices are formed behind the cylinder at extreme positions.
4) The integrated streakline patterns show a pronounced kink of the tail generated immediately behind the trailing edge.
5) In all cases, an integrated streakline is shed from a point near the trailing edge.

5. Acknowledgements

The authors would like to express their sincere thanks to Dr. H. Honji for his stimulating discussion and interest in this work. They also owe thanks to Mr. K. Ishi-i for his always obligingness and assistance in

carrying out the experiment. This work was supported by the Grant-in-Aid from the Ministry of Education, Science and Culture.

REFERENCES

1) Taneda, S. : Progress in Aerospace Science, **17** (1977) 287.
2) Honji, H. : Rep. Res. Inst. Appl. Mech., **XIX** No. 65 (1972) 271.
3) Lugt, H. J., Obring, S. : J. Fluid Mech., **65** (1974) 711.
4) Lugt, H. J., Haussling, H. J. : J. Fluid Mech., **79** (1977) 124.
5) Okajima, A., Takata, H., Asanuma, T. : Inst. Space and Aero. Sci. Univ. Tokyo Rep. No. 533 (1975) 339.
6) Tatsuno, M.: Rep. Res. Inst. Appl. Mech., **XXVI** No.85 (1979) 99.
7) Moore, F.K. : *Boundary Layer Research*, edited by H. Görtler, (Springer, Berlin, 1958) p. 296.
8) Rott, N. : Quarterly Journal of Applied Mathematics, **13** (1956) 444.
9) Sears, W.R. : Journal of Aerospace Science, **23** No.5 (1956) 490.
10) Taneda, S., Honji, H., Tatsuno, M. : International Symposium on Flow Visualization, (1977) 133.

(Received June 30, 1980)

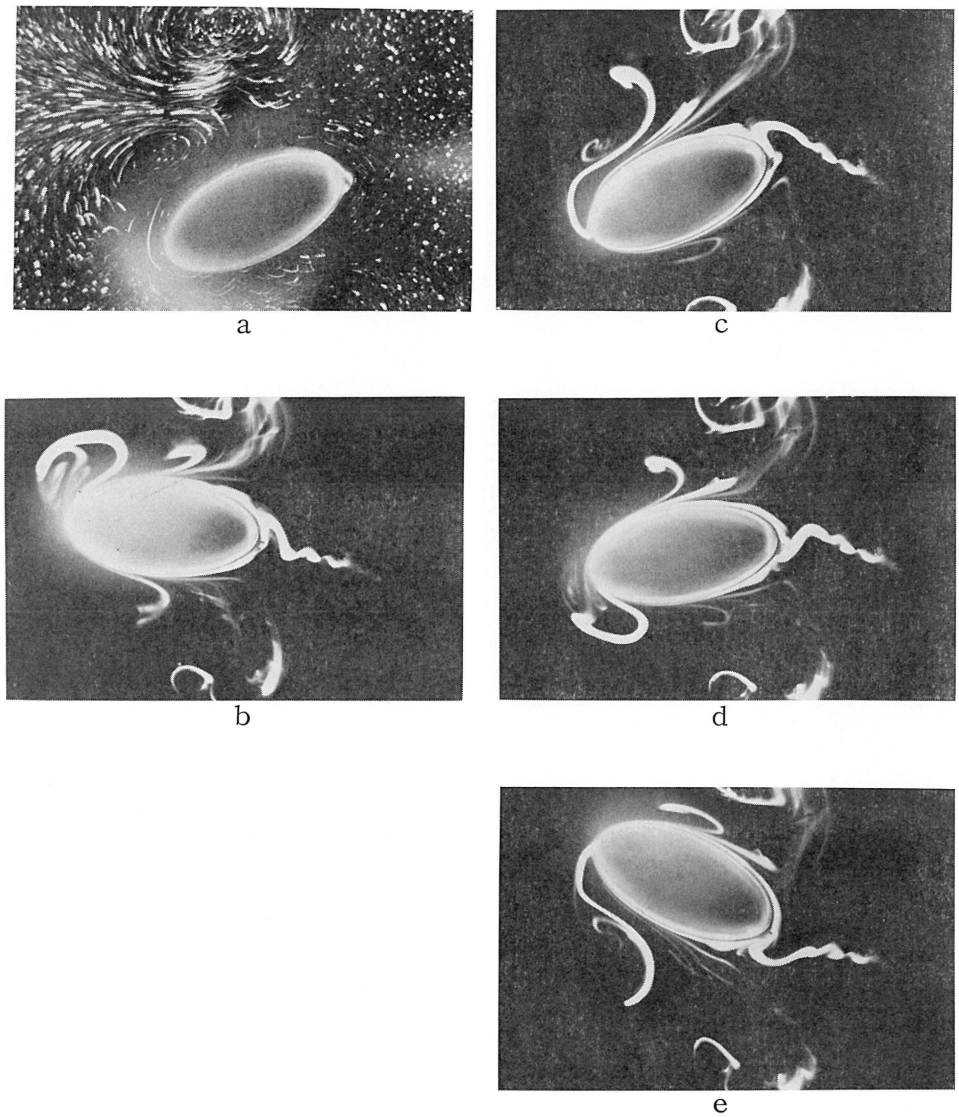

Fig. 4. Streamline patterns and the corresponding streakline patterns around the oscillating elliptic cylinder.
a=3.0 cm, b=1.5 cm, N=0.1 Hz, U=0.0 cm/s, θ=30°,
ν=0.011 cm²/s, R_e=0.0, S_t=infinity
a) t=36.3 s α= −30°
b) t=44.2 s α= 0°
c) t=47.0 s α= −30°
d) t=49.2 s α= 0°
e) t=51.8 s α= 30°

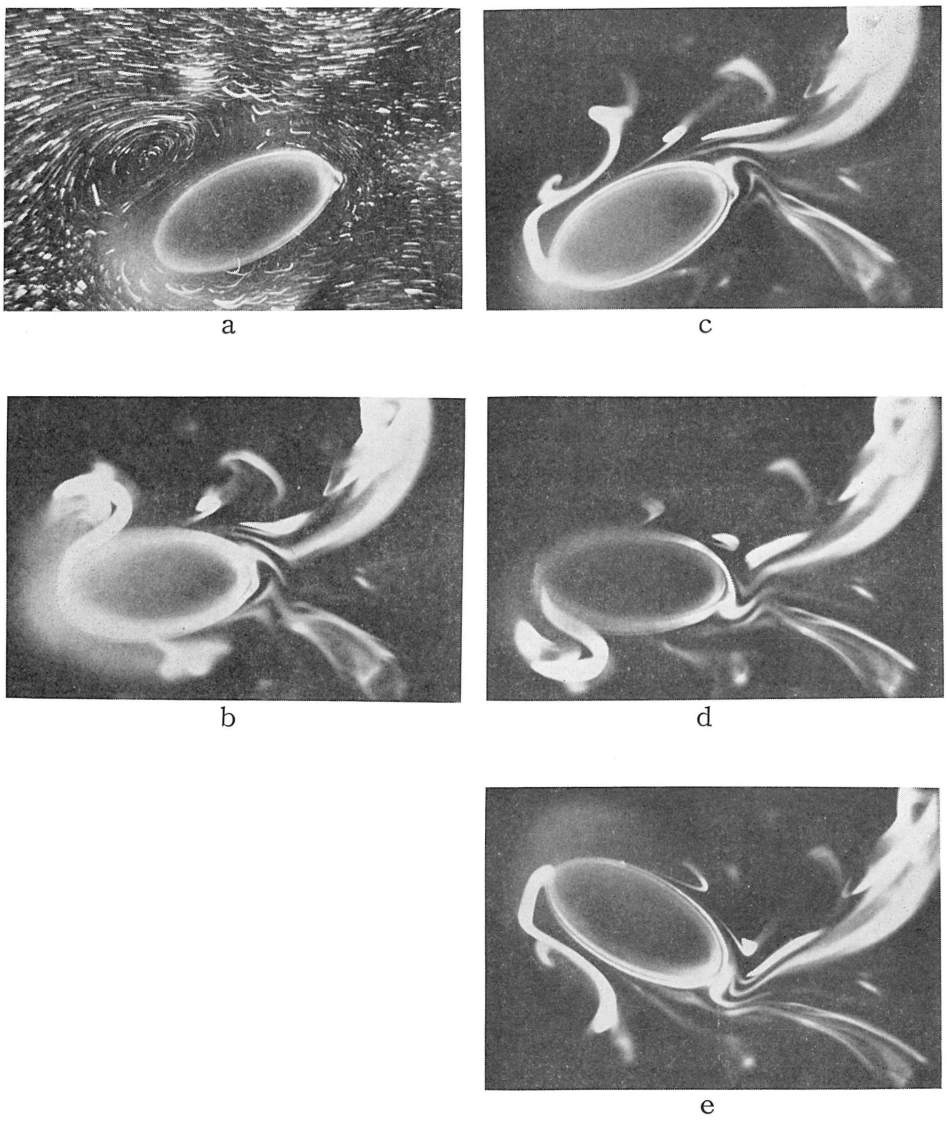

Fig. 5. $a=3.0$ cm, $b=1.5$ cm, $N=0.1$ Hz, $U=0.126$ cm/s, $\theta=30°$, $\nu=0.011$ cm^2/s, $R_e=34.4$, $S_t=2.38$

a) $x/a=1.35$ $\alpha=-30°$
b) $x/a=1.90$ $\alpha=0°$
c) $x/a=1.98$ $\alpha=-30°$
d) $x/a=2.10$ $\alpha=0°$
e) $x/a=2.20$ $\alpha=30°$

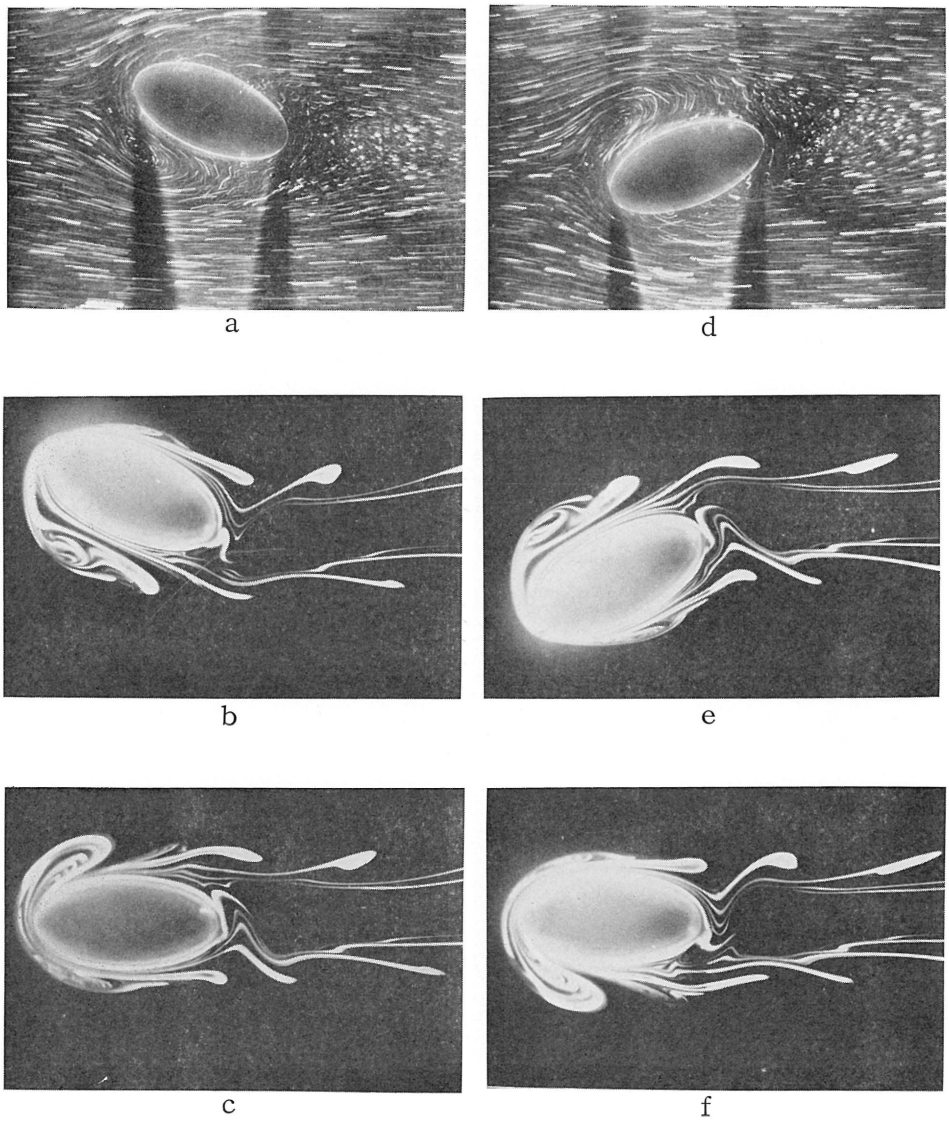

Fig. 6. $a=3.0$ cm, $b=1.5$ cm, $N=0.1$ Hz, $U=0.259$ cm/s, $\theta=30°$, $\nu=0.011$ cm^2/s, $R_e=70.6$, $S_t=1.15$

a) $x/a=9.64$ $\alpha=30°$
b) $x/a=5.37$ $\alpha=30°$
c) $x/a=5.57$ $\alpha=0°$
d) $x/a=10.07$ $\alpha=-30°$
e) $x/a=5.81$ $\alpha=-30°$
f) $x/a=6.02$ $\alpha=0°$

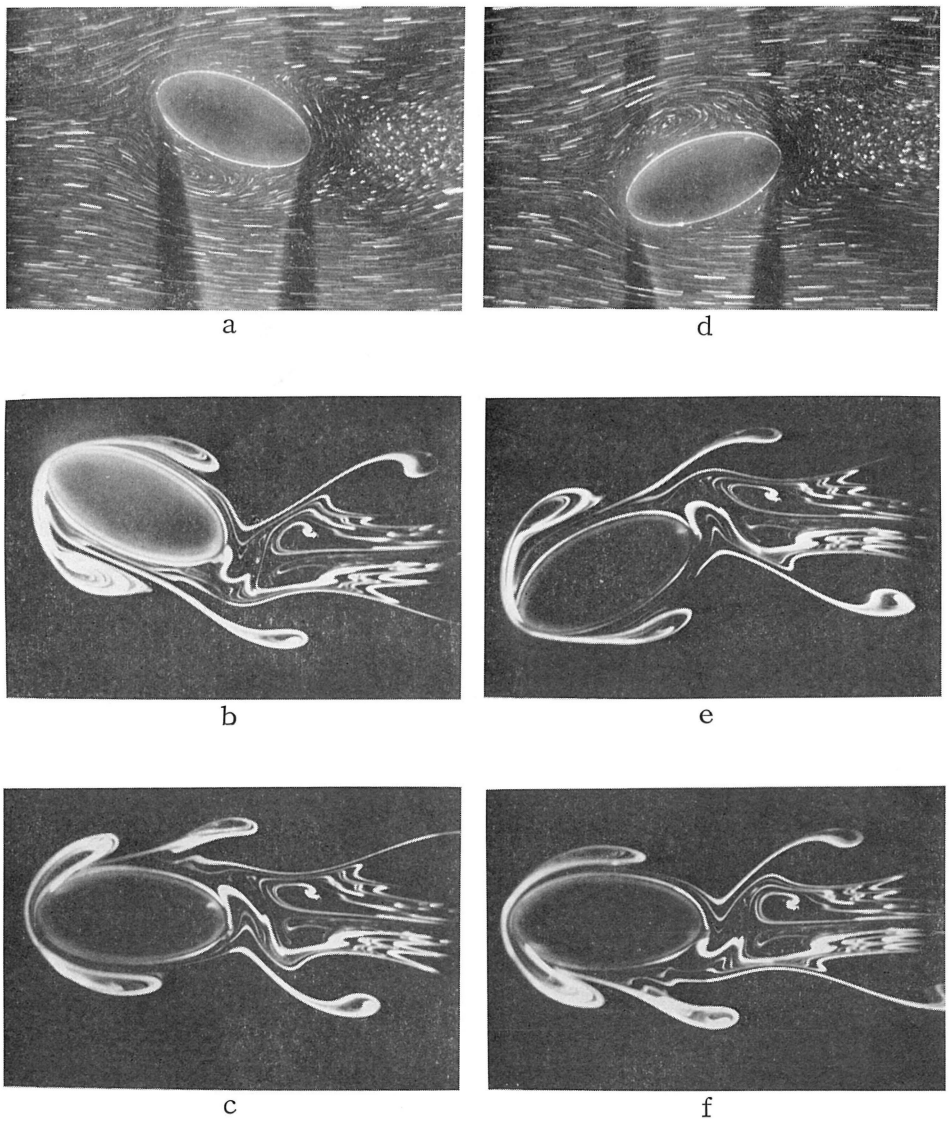

Fig. 7. $a=3.0$ cm, $b=1.5$ cm, $N=0.1$ Hz, $U=0.5$ cm/s, $\theta=30°$, $\nu=0.011$ cm^2/s, $R_e=136.8$, $S_t=0.6$

a) $x/a=22.83$, $\alpha=30°$
b) $x/a=18.67$, $\alpha=30°$
c) $x/a=19.08$, $\alpha=0°$
d) $x/a=23.50$, $\alpha=-30°$
e) $x/a=19.55$, $\alpha=-30°$
f) $x/a=19.95$, $\alpha=0°$

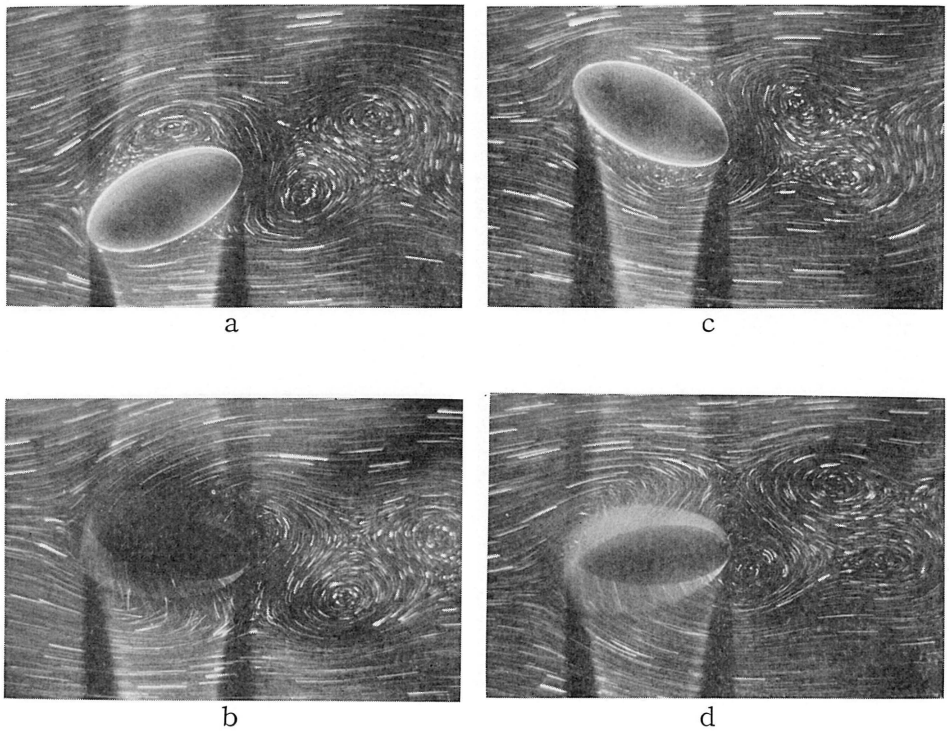

Fig. 8.1 Streamline Patterns
$a=3.0$ cm, $b=1.5$ cm, $N=0.1$ Hz, $U=0.757$ cm/s,
$\theta=30°$, $\nu=0.011$ cm^2/s, $R_e=206.5$, $S_t=0.396$
a) $x/a=23.21$, $\alpha=-30°$
b) $x/a=23.92$ $\alpha=0°$
c) $x/a=24.58$ $\alpha=30°$
d) $x/a=25.18$ $\alpha=0°$

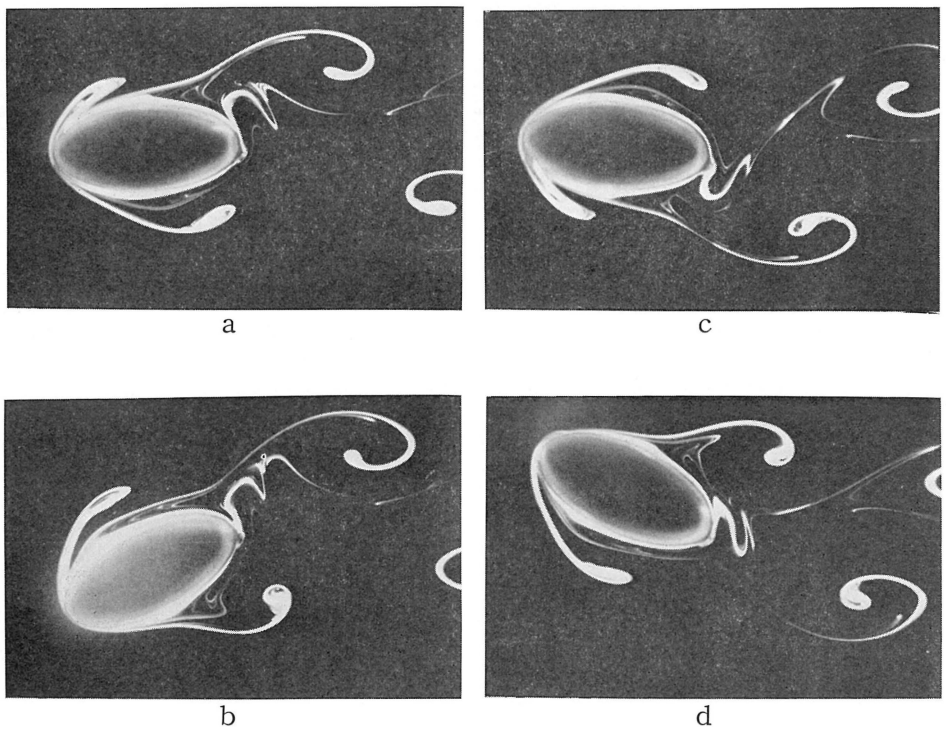

Fig. 8.2 Streakline Patterns
$a=3.0$ cm, $b=1.5$cm, $N=0.1$ Hz, $U=0.757$ cm/s,
$\theta=30°$, $\nu=0.011$ cm^2/s, $R_e=206.5$, $S_t=0.396$

a) $x/a=24.02$ $\alpha=\ 0°$
b) $x/a=24.52$ $\alpha=-30°$
c) $x/a=25.33$ $\alpha=\ 0°$
d) $x/a=26.04$ $\alpha=\ 30°$

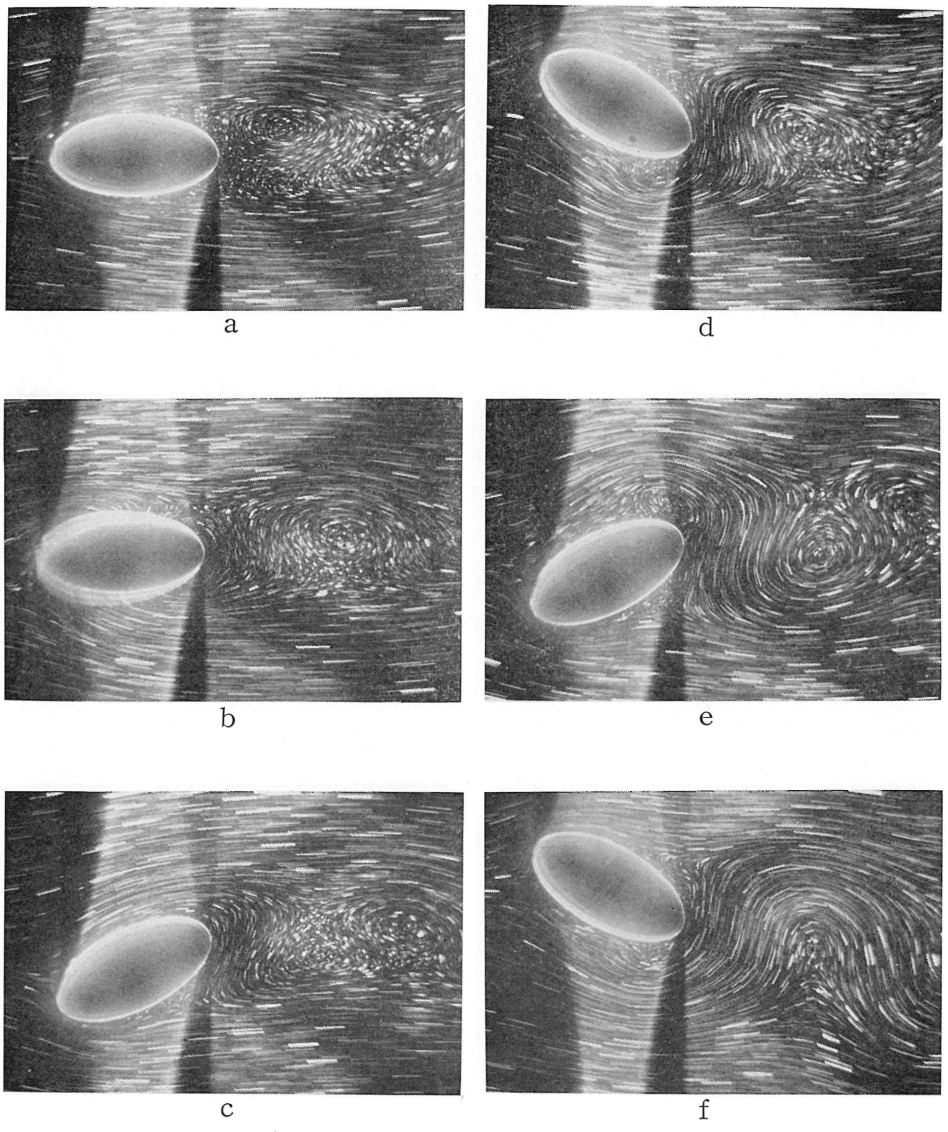

Fig. 9. Streamline patterns from start of oscillation to some later time.
$a=3.0$ cm $b=1.5$ cm, $N=0.1$ Hz, $U=1.0$ cm/s, $\theta=30°$,
$\nu=0.011$ cm^2/s, $R_e=272.7$, $S_t=0.3$

a) $x/a=0.0$ $\alpha=\ 0°$
b) $x/a=0.1$ $\alpha=-\ 4°$
c) $x/a=0.83$ $\alpha=-30°$
d) $x/a=2.5$ $\alpha=\ 30°$
e) $x/a=4.17$ $\alpha=-30°$
f) $x/a=5.83$ $\alpha=\ 30°$

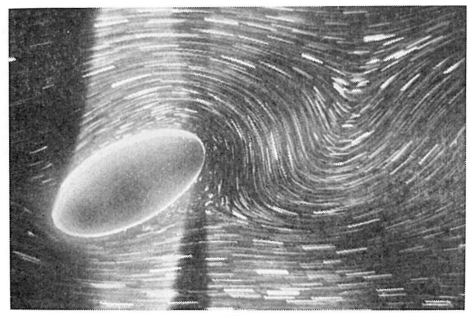
g

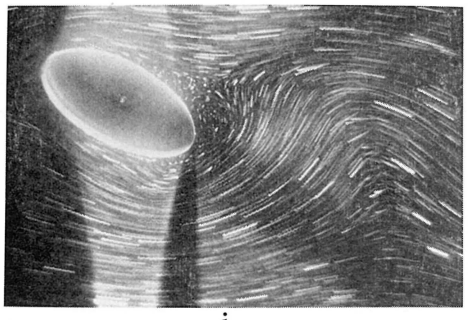
j

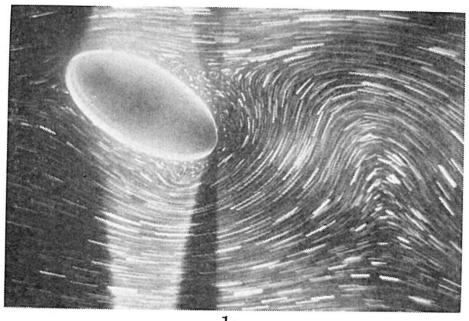
h

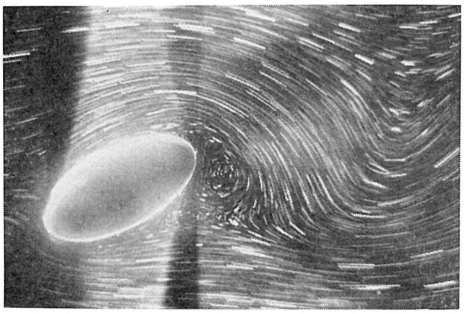
k

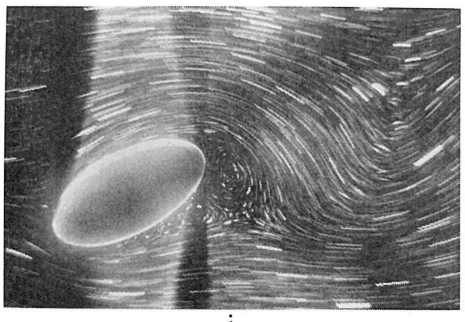
i

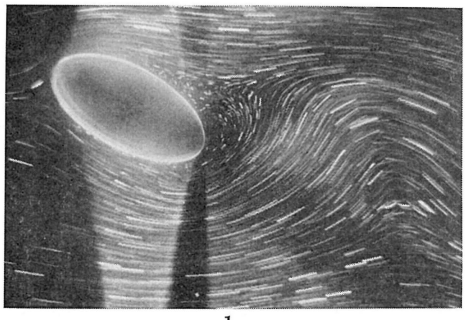
l

Fig. 9. Continue

g) $x/a=7.5$ $\alpha=-30°$
h) $x/a=9.17$ $\alpha=30°$
i) $x/a=10.83$ $\alpha=-30°$
j) $x/a=12.5$ $\alpha=30°$
k) $x/a=14.17$ $\alpha=-30°$
l) $x/a=15.83$ $\alpha=30°$

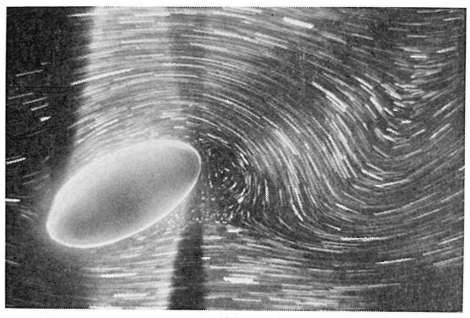

m

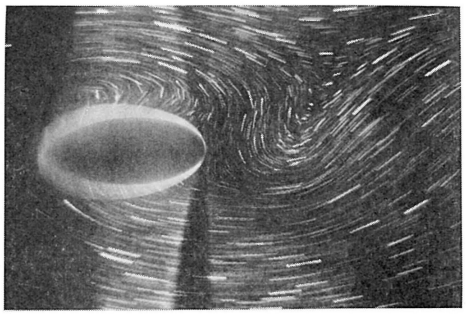

o

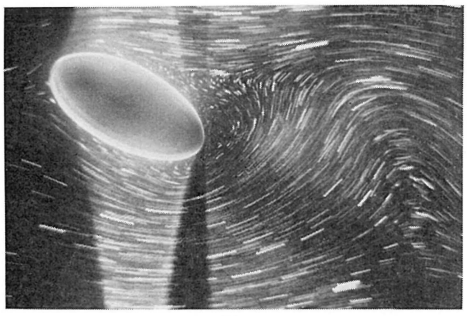

n

Fig. 9 Continue

m) $x/a=17.5$ $\alpha=-30°$
n) $x/a=19.17$ $\alpha=30°$
o) $x/a=26.67$ $\alpha=0°$